Pharm Res (2014) 31:649–659
DOI 10.1007/s11095-013-1187-0

RESEARCH PAPER

Bayesian Approach to Estimate AUC, Partition Coefficient and Drug Targeting Index for Studies with Serial Sacrifice Design

Tianli Wang • Kyle Baron • Wei Zhong • Richard Brundage • William Elmquist

Received: 14 May 2013 / Accepted: 9 August 2013 / Published online: 3 October 2013

ABSTRACT

Purpose The current study presents a Bayesian approach to non-compartmental analysis (NCA), which provides the accurate and precise estimate of AUC_0^{∞} and any AUC_0^{∞} -based NCA parameter or derivation.

Methods In order to assess the performance of the proposed method, 1,000 simulated datasets were generated in different scenarios. A Bayesian method was used to estimate the tissue and plasma AUC_0^{∞} s and the tissue-to-plasma AUC_0^{∞} ratio. The posterior medians and the coverage of 95% credible intervals for the true parameter values were examined. The method was applied to laboratory data from a mice brain distribution study with serial sacrifice design for illustration.

Results Bayesian NCA approach is accurate and precise in point estimation of the AUC_0^{∞} and the partition coefficient under a serial sacrifice design. It also provides a consistently good variance estimate, even considering the variability of the data and the physiological structure of the pharmacokinetic model. The application in the case study obtained a physiologically reasonable posterior distribution of AUC, with a posterior median close to the value estimated by classic Bailer-type methods.

Conclusions This Bayesian NCA approach for sparse data analysis provides statistical inference on the variability of AUC_0^{∞}-based parameters such as partition coefficient and drug targeting index, so that the comparison of these parameters following destructive sampling becomes statistically feasible.

KEY WORDS Bayesian approach · drug targeting index · NCA · partition coefficient · variance estimation

ABBREVIATIONS

AUC	Area under the concentration-time curve
AUC_0^t	AUC from time zero to the last time point
AUC_0^{∞}	AUC from time zero to infinity
a, b, c	Large positive numbers in the prior settings indicating vague priors
BAV	Between-animal coefficient of variation
BCRP	Breast cancer resistance protein
BCRPKO	BCRP gene knockout (*Bcrp1 (-/-)*)
br	The brain or any other tissue
C.I.	Credible interval
C.I.*	Confidence interval
$\overrightarrow{C_{ij}}$	Plasma and tissue concentrations of the i^{th} animal at the j^{th} time point
C_j	Concentration at the j^{th} time point
C_j*	Concentrations at the last three sampling time points
C_t	Concentration at the last sampling time point
d	Degree of freedom
DTI	Drug targeting index
i	Animal indicator
j	Time point indicator
k, θ	Superparameters of an Inverse-Gamma distribution
MVN (·,·)	Multivariate normal distribution
m	The total number of sampling time points
n	Number of animals at each time point
N (·,·)	Normal distribution
NCA	Noncompartmental analysis
P-gp	P-glycoprotein
PgpKO	P-gp gene knockout (*Mdr1a/b (-/-)*)
pl	The plasma
R	Two-dimensional scale matric for Inverse-Wishart distribution
SD	Standard deviation

Electronic supplementary material The online version of this article (doi:10.1007/s11095-013-1187-0) contains supplementary material, which is available to authorized users.

T. Wang • W. Elmquist (✉)
Department of Pharmaceutics, University of Minnesota
308 Harvard St. SE, Minneapolis, Minnesota 55455, USA
e-mail: elmqu011@umn.edu

K. Baron • W. Zhong • R. Brundage
Department of Experimental and Clinical Pharmacology
University of Minnesota, Minneapolis, Minnesota, USA

SE_j	Standard error of C_j
t_j	Time corresponding to the j^{th} time point
t_j *	Time corresponding to the last three time points in a concentration-time profile
TKO	Triple knockout (*Mdr1a/b (-/-)Bcrp1 (-/-)*)
Unif	Uniform distribution
WAV	Within-animal variability
WT	Wild-type
λ_z	The terminal elimination rate constant
μ_j	Mean of the log-transformed concentrations at the jth time point
$\vec{\mu}_j$	The vector $(\mu_{pl,j}\ \mu_{br,j})^T$
Σj	Within-animal precision variance-covariance matrix of concentrations at time j
σ_j	Variance or covariance of the plasma and brain concentrations at the jth time point
σ*	Standard deviation of the log-normal distribution of concentrations at the last three time points of a concentration-time profile
α	The intercept for the terminal phase regression
β	The slope for the terminal phase regression

INTRODUCTION

In preclinical studies, the partition coefficient or so-called equilibrium-distribution coefficient, expressed by the ratio of tissue-to-plasma area under the concentration curve (AUC) from time zero to infinity ($\frac{AUC^{\infty}_{0,br}}{AUC^{\infty}_{0,pl}}$, where the subscript *br* denotes the brain or any other tissue under investigation and *pl* denotes the plasma), has been widely used as a key metric to reflect the tissue distribution of a compound (1,2). For instance, when the compound under investigation is a substrate of the blood–brain barrier (BBB) efflux transporter system, it is becoming increasingly important to characterize the brain-to-plasma partition coefficient in order to assess the brain penetration of the compound in drug discovery (3). The ratio of AUC from time zero to infinity (AUC_0^{∞}) is also of primary importance in bioequivalence studies. In addition, the drug targeting index (DTI, the ratio of AUC_0^{∞} at target and systemic site following administration into and sampling from both sites) is widely used in regional drug delivery research (4,5). Nevertheless, to determine the true tissue-to-plasma AUC_0^{∞} ratio or the true DTI is usually not straightforward due to experimental error and the variation between animals.

In order to obtain the statistical inference of AUC_0^{∞}, it is ideal to perform intensive serial sampling in each individual animal. However, the withdrawal of a sufficient number of blood samples from individual rodents for AUC determination is restricted due to technical and financial reasons. A common scenario in preclinical pharmacokinetic studies with small animals is the use of a sparse sampling approach with few time points, in which each animal is not sampled at all time points. Typically, in a serial sacrifice design (or so-called "destructive sampling"), only one sample per animal is available (6). In this experimental scenario, more challenges arise in the estimation of AUC_0^{∞} variance than in the intensive sampling design. Accordingly, it is even more difficult to make the statistical inference of the partition coefficient and DTI.

Under serial sacrifice design, there is theoretically no correlation in drug concentrations between different time points, however, the correlation between the tissue and the plasma concentrations within an animal cannot be ignored (see Fig. 1). The occurrence of plasma and tissue correlation at each time point further complicates the estimation of the variability around $\frac{AUC^{\infty}_{0,br}}{AUC^{\infty}_{0,pl}}$. As far as we know, no conventional method provides solutions with the correlation taken into account.

In recent years, Bayesian approaches have been widely applied to clinical trials (7–10) and pharmacokinetic (PK) & pharmacodynamic studies (11,12). Unlike the frequentist view that the conclusions made from the current work are independent of prior work, the Bayesian approach acknowledges that parameters are random variables that follow an unknown distribution instead of fixed constants, and that existing knowledge could be incorporated into the analysis as an informative prior, if any. The priors in Bayesian statistics reflect the investigator's beliefs in specific parameters before the beginning of the study and the Bayesian approach allows estimation of a parameter of interest by incorporating existing knowledge. When there is little or no prior information available, a non-informative prior can be used. The posterior distribution of a certain parameter is derived *via* the simulation-based method, with the knowledge of prior distribution of the parameter estimates and the actual data. Bayesian methods implement a simulation-based approach to obtain the point estimate of posterior expectation and any quantile of interest, and it is applicable for sparse sampling data. The most pertinent advantage of this proposed approach is the ability in estimating the uncertainty of any noncompartmental analysis (NCA) parameter through the posterior samplings of the mean concentration at each time point.

The current study presents a novel Bayesian NCA approach using the BUGS (Bayesian inference Using Gibbs Sampling) software, which provides the posterior distributions of not only the AUC_0^{∞} but also of the AUC_0^{∞} ratio and the DTI. Since no prior information was used in our study, non-informative or vague prior distributions were assumed for all model parameters.

THEORY

Bailer's method was first proposed and has been most commonly used to estimate the AUC from time zero to the last sampling

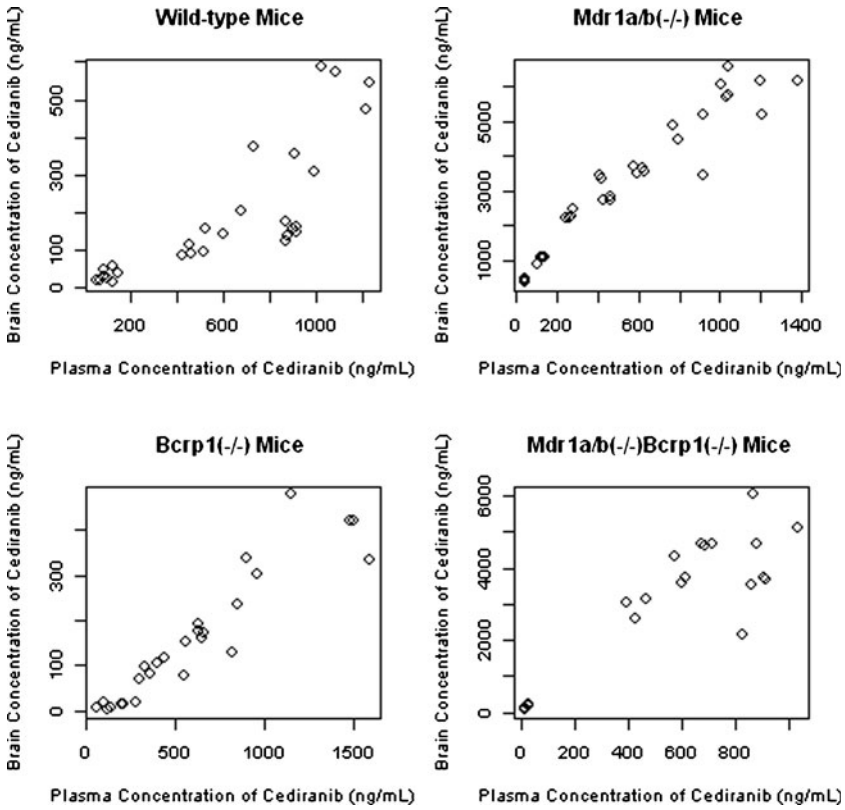

Fig. 1 Correlation between plasma and brain concentrations after intravenous injection of 4 mg/kg cediranib into four genotypes of FVB mice: wild-type, *Mdr1a/b (-/-)*, *Bcrp1 (-/-)* and *Mdr1a/b (-/-) Bcrp1 (-/-)*.

time point (AUC_0^t) based on the linear trapezoidal rule. The corresponding variance of the estimated AUC_0^t was calculated based on the linear relation of normally distributed sample errors of concentration at each time point (13). Bailer-Satterwaite method improves the accuracy of the population variance estimation by the Bailer's method when sample sizes are not adequately large, and expands the Bailer's method for AUC confidence intervals in sparse sampling (14). However, in a study under serial sacrifice design, Bailer-Satterwaite method was still unable to obtain the variance of the AUC_0^∞, as described as follows:

$$AUC_0^\infty = AUC_0^t + \frac{C_t}{\lambda_z}, \tag{1}$$

where C_t represents the concentration at the last sampling time point, and λ_z denotes the terminal elimination rate constant that can be estimated by the linear regression from the logarithm of concentrations at the last at lease three sampling points.

Now the question at hand is how to estimate the variance of AUC_0^∞, and further conduct contrasts between different AUC_0^∞s. Yuan extends the Bailer's method to infinite time and construct confidence intervals for AUC_0^∞ (15). Yuan's method proposed the following approximation for the variability of AUC_0^∞ by assuming that all the samples are independent and that λ_z is known and identical for all tested animals:

$$SD\left(AUC_0^\infty\right) = \sqrt{\left(1\Big/2(t_1-t_0)SE_0\right)^2 + \sum_{j=2}^{m}\left(1\Big/2\left(t_j-t_{j-2}\right)SE_{j-1}\right)^2 + \left(1\Big/2(t_m-t_{m-1}) + \frac{1}{\lambda_z}\right)^2 SE_m^2}, \tag{2}$$

where SD(·) denotes the standard deviation; SE_j is the standard error of C_j, the concentration at the j^{th} time point; SE_0 denotes the standard error of the concentrations at time zero; the subscript m is the total number of sampling time points; and the λ_z represents the terminal rate constant. Yuan also pointed out that because of the covariance between the mean concentration at the j^{th} time point and λ_z , Eq. 2 underestimated the variation of AUC_0^∞. It was proposed that

one more term should be added to the variance of AUC_0^{∞} if λ_z is estimated from an independent study. However, it is usually hard to fulfill in practice. Thus, Yuan's method also has some inherent limitations because of its assumptions. Moreover, one problem not addressed in Yuan's method is the estimation of the variance of partition coefficient, and therefore the variance of DTI, which requires more strict statistical assumptions and complicated mathematical computation.

Alternatively, resampling-based approaches have become an option to obtain the non-parametric confidence intervals of AUC_0^{∞} or AUC_0^{∞} *via* bootstrapping and jackknifing (6,16–19). However, the sample size for resampling is an important issue to consider when using these methods (16,20). The coverage rate of resampling-based approaches is a concern, especially for bootstrap. The biggest disadvantage of resampling-based approaches is that it provides no guarantees on general finite-sample and tends to be overly optimistic, which makes its application on sparse sampling designs questionable (16).

Here in this paper, we proposed a Bayesian approach to estimate the variance of AUC_0^{∞} and AUC_0^{∞}-based parameters such as partition coefficient and DTI. The Bayesian approach is based on the conventional method of AUC_0^{∞} calculation (Eq. 1). The main difference from conventional methods is that the model based-mean concentrations at the different time points are used for AUC calculation. The Bayesian NCA approach presented here includes the following statistical assumptions:

Likelihood

Assume the plasma and the tissue (*e.g.*, the brain, in this paper) concentration measurements were obtained on the i^{th} animal at the j^{th} sampling time as $\vec{C}_{ij}$ (or $C_{pl,ij}$ and $C_{br,ij}$, respectively). For each sampling time point, there were n animals for sample collection. Log-normality was assumed for the individual-specific PK measurement $\vec{C}_{ij}$.

$$\ln\vec{C}_{ij} \sim MVN(\vec{\mu}_j, \Sigma_j), \tag{3}$$

Or explicitly,

$$\left(\ln C_{pl,ij}, \ln C_{br,ij}\right) \sim MVN\left(\begin{bmatrix}\mu_{pl,j}\\ \mu_{br,j}\end{bmatrix}, \begin{bmatrix}\sigma^2_{pl,j} & \sigma_{br,pl,j}\\ \sigma_{pl,br,j} & \sigma^2_{br,j}\end{bmatrix}\right), \tag{4}$$

where MVN $(\cdot,\cdot)$ denotes a bivariate normal distribution. $\vec{\mu}_j$ is a vector with two components ($\mu_{pl,j}$ and $\mu_{br,j}$), representing means of the log-transformed plasma and brain concentrations ($C_{pl,ij}$ and $C_{br,ij}$), respectively. Σj is the within-animal precision matrix of concentrations at the j^{th} time point; and σ_j denotes the variance of the plasma or brain concentrations or covariance of the plasma and brain concentrations at the j^{th} time point. With the precision matrix, the correlation between $C_{pl,ij}$ and $C_{br,ij}$ was taken into account in model setting, which could improve the precision of estimate.

Prior Specification

A non-informative (vague) prior distribution model was constructed in the absence of prior knowledge about model parameters. The prior distributions of $\mu_{pl,j}$ and $\mu_{br,j}$ were assumed as uniform distributions (Unif) in a wide range, for instance,

$$\mu_{pl,j} \sim Unif(-a, a), \quad \mu_{br,j} \sim Unif(-a, a), \tag{5}$$

where a is a large positive number indicating vague priors.

Typically, prior distributions of parameters are specified for mathematical convenience to compute posteriors. Thus, the inverse of the variance-covariance matrix (Σ^{-1}), or so-called precision matrix, was set as a 2-dimensional Wishart distribution, a probability distribution of random nonnegative-definite symmetric matrices. Accordingly, the variance-covariance matrix of concentrations at the j^{th} time point (Σj) follows an Inverse-Wishart distribution as follow,

$$\Sigma_j \sim Inverse - Wishart(R, d), \tag{6}$$

where R is a two-dimensional scale matrix; d is the degree of freedom. By setting small values as the diagonal elements of R (*e.g.*, 0.01) and the degree of freedom (*e.g.*, 2), vague priors for the correlation parameters were used.

$$R = \begin{bmatrix}0.01 & 0\\ 0 & 0.01\end{bmatrix}$$

METHOD

The two Markov chain Monte Carlo (MCMC) chains were generated by OpenBUGS version 3.2.2 (www.mrc-bsu.cam.ac.uk/bugs/welcome.shtml) to obtain the posterior samples. To ensure that stationary distributions for the parameters were achieved, the first 10,000 samples for each chain were discarded (termed "burn-in period") and the following 20,000 samples were retained for inference. Sampler convergence was assessed by visual inspection of the trace plot (*i.e.*, plotting the draw of the parameter against iteration number for each Markov chain), autocorrelation, and the Gelman–Rubin diagnostic for each parameter. The median of the posterior samples (the 50th percentile) and 95% credible interval (C. I., the range from the 2.5th to 97.5th percentile) were summarized.

The Calculation of AUC and Terminal Elimination Rate Constant

Parameters such as AUC and the brain-to-plasma AUC ratio were estimated within a Bayesian framework using R-package "BRugs" version 0.8-1 (21). In the current study, even though we could incorporate prior information into the analysis, we used non-informative priors throughout. Both brain and plasma $AUC_0{}^t$ were calculated from model-based mean concentrations by the trapezoidal rule. Equation 1 shows that $AUC_0{}^\infty$ is the sum of $AUC_0{}^t$ and C_t/λ_z. Thus it was desirable to determine the terminal elimination rate constant λ_z to calculate AUC from the last sampling time to infinity.

By assuming a first-order elimination process at terminal phase including the last three time points (t_{j*}) in the current study, the terminal elimination rate constant λ_z can be estimated using linear regression on the naturally-log-transformed concentrations at the last three time points (C_{j*}), which yields a log-normal likelihood as shown below.

$$ln\,C_{j*} \sim N\left(\alpha - \beta \cdot t_{j*}, \sigma^{*2}\right), \tag{7}$$

where $N(\alpha-\beta\cdot t_{j*},\sigma^{*2})$ denotes a normal distribution with the mean $(\alpha-\beta\cdot t_{j*})$ and standard deviation σ^*; α is the intercept term and the slope term β defines the terminal elimination rate constant λ_z. The priors for α and β were assumed to follow the following uniform distributions:

$$\alpha \sim Unif(-b, b), \qquad \beta \sim Unif(0, c), \tag{8}$$

where b and c were large positive values indicating vague priors.

Similar to the variance-covariance matrix Σj as described in the "Theory" section, an inverse-gamma prior was specified for σ^{*2}, which is also the standard conjugate prior for the normal variance for computing convenience. The superparameters of k and θ in the inverse-gamma distribution (Inverse-Gamma (k, θ)) were set to be 0.01 to ensure "vague" priors:

$$\sigma^{*2} \sim Inverse-Gamma(0.01, 0.01). \tag{9}$$

SIMULATION

In order to examine the precision and coverage by Bayesian approach in estimation of the $AUC_0{}^\infty$ and the tissue-to-plasma partition coefficient, we applied the proposed Bayesian NCA method to 1,000 sets of simulated data with serial sacrifice design, and compared the obtained results with nominal values of the parameters. The experiment was simulated in R (Version 2.12.0) (22) and two scenarios were investigated: animals with tissue-compartment efflux transporter activity and animals without tissue-compartment efflux transporter activity. Sampling from 28 animals was simulated at 7 arbitrary time points (4 animals per time point) following a serial sacrifice design. The time points were set to be 0.5, 1, 2, 4, 8, 16, 24 h after the dose. A two-compartment PK model consisting of the plasma compartment and the tissue compartment was assumed (Fig. 2). A single i.v. bolus dose of 1,000 units was given to the plasma compartment at time zero. Arbitrary PK parameters were defined in Table I. A 5-fold transporter-mediated increase in clearance out of the tissue compartment was simulated with the expected $\frac{AUC^{\infty}_{0,br}}{AUC^{\infty}_{0,pl}}$ ratio of 0.2. Note that the PK model does not include saturation of the transporter activities. Log-normally distributed between-animal variability (BAV) and proportional residual variability (or so-called within animal variability, WAV) were incorporated. For each simulated dataset, the posterior medians of $AUC^{\infty}_{0,pl}$, $AUC^{\infty}_{0,br}$ and $\frac{AUC^{\infty}_{0,br}}{AUC^{\infty}_{0,pl}}$ along with 95% Bayesian credible intervals were obtained. The estimations were compared to the true parameter values. The results by the proposed method were assessed when data have different levels of variability (5% BAV + 5% WAV; 10% BAV + 10% WAV; 20% BAV + 10% WAV; or 20% BAV + 20% WAV).

CASE STUDY

The Bayesian method was applied to and evaluated in a real-world animal experiment. Briefly, brain and plasma levels of cediranib were determined following intravenous injection into wild-type (WT), P-glycoprotein (P-gp) gene-knockout (PgpKO or *Mdr1a/b (-/-)*), breast cancer resistance protein (BCRP) gene-knockout (BCRPKO or *Bcrp1 (-/-)*), and P-gp and BCRP triple gene-knockout (TKO or *Mdr1a/b (-/-) Bcrp1 (-/-)*) mice (23). In this experiment, cediranib concentrations were assumed to be normally distributed. In order to explore whether the absence of P-gp or BCRP changes the blood–brain barrier transport of cediranib, the brain-to-plasma partition coefficient (*i.e.*, $\frac{AUC^{\infty}_{0,br}}{AUC^{\infty}_{0,pl}}$) and the DTI $\frac{\left(\frac{AUC^{\infty}_{0,br}}{AUC^{\infty}_{0,pl}}\right)_{transgenic\cdot mice}}{\left(\frac{AUC^{\infty}_{0,br}}{AUC^{\infty}_{0,pl}}\right)_{wildtype\cdot mice}}$

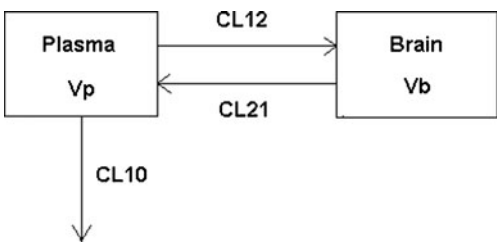

Fig. 2 Simulated two-compartment PK model.

Table I Model Parameters of the Simulated Two-compartment Model

Parameter	Population parameter value	Between-animal variability
Scenario 1: No efflux transporter activity		
Vp	50	Yes
Vb	50	No
CL12	10	Yes
CL21	10	Yes
CL10	20	Yes
Scenario 2: High efflux transporter activity		
Vp	50	Yes
Vb	50	No
CL12	10	Yes
CL21	50	Yes
CL10	20	Yes

are the variables of interests for statistical comparison among the four genotypes. The posterior medians with 95% credible intervals for the $\frac{AUC^{\infty}_{0,br}}{AUC^{\infty}_{0,pl}}$ in different genotypes were obtained by utilizing the Bayesian approach. The posterior median and 95% credible interval of the plasma and brain AUC^{∞}_{0} in different genotypes were compared with the point estimate and 95% confidence interval (C. I. *) approximated by Yuan's method utilizing Eq. 2 and with the mean and 95% confidence interval obtained with the jackknife resampling approach performed in R (resampling times = 1,000). The posterior medians with 95% credible intervals for the $\frac{AUC^{\infty}_{0,br}}{AUC^{\infty}_{0,pl}}$ for different genotypes were also compared with jackknife mean and 95% confidence intervals. In order to evaluate the performance of Bayesian method and compare it with the Bailer-Satterthwaite method, the posterior medians and 95% Bayesian credible intervals of the plasma and brain AUC^{t}_{0} were also computed and compared with the estimators obtained with Phoenix WinNonlin® 6.1 (Mountain View, CA) utilizing the Bailer-Satterthwaite method (14,24).

RESULTS

Simulation with Serial Sacrifice Design

Standard convergence diagnostics described in the "Method" section did not reveal significant MCMC convergence issues. Figure 3 illustrates the posterior median distributions for $AUC^{\infty}_{0,pl}$, $AUC^{\infty}_{0,br}$ and $\frac{AUC^{\infty}_{0,br}}{AUC^{\infty}_{0,pl}}$ based on the 1,000 simulated data sets for two extreme scenarios with and without tissue efflux transporter activity with high variability (*e.g.*, 20% BAV + 20% WAV). The posterior medians of the three parameters were close to the preset true population mean. The mean of the posterior medians for $AUC^{\infty}_{0,pl}$, $AUC^{\infty}_{0,br}$ and $\frac{AUC^{\infty}_{0,br}}{AUC^{\infty}_{0,pl}}$ based on the 1,000 simulated datasets are shown in Table II, for both transporter activity scenarios. The posterior median was used as an estimator to compare with the true parameter since the log-normal distribution is right-skewed. Interestingly, the estimation for $\frac{AUC^{\infty}_{0,pl}}{AUC^{\infty}_{0,pl}}$ was even of higher accuracy (bias ≤5%) than the estimation for $AUC_{0,\,pl}{}^{\infty}$ (bias <20%). The

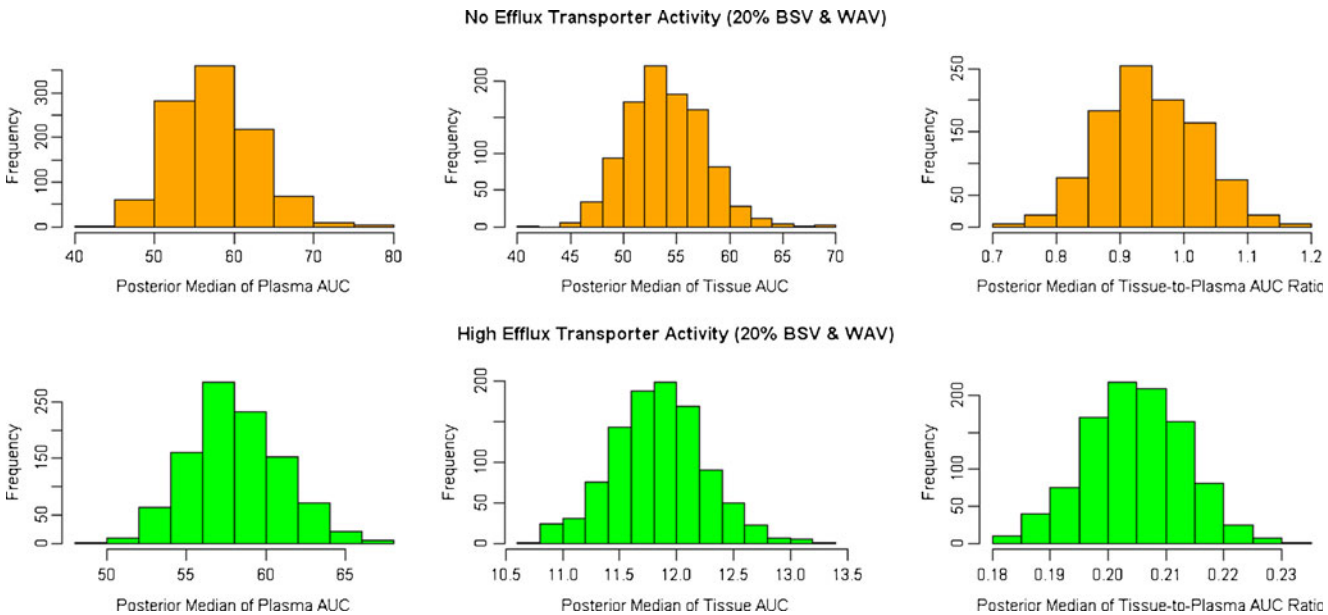

Fig. 3 Posterior median distributions for $AUC^{\infty}_{0,pl}$, $AUC^{\infty}_{0,br}$ and $\frac{AUC^{\infty}_{0,br}}{AUC^{\infty}_{0,pl}}$ based on the 1,000 simulated data sets for two extreme scenarios with and without tissue efflux transporter activity with high variability.

Table II Evaluation of the Robustness of Posterior Estimators of $AUC^{\infty}_{0,pl}$, $AUC^{\infty}_{0,br}$ and $\frac{AUC^{\infty}_{0,br}}{AUC^{\infty}_{0,pl}}$ Obtained by the Bayesian NCA Approach Based on 1,000 Monte Carlo Simulations

	Parameter	Nominal population mean	Averaged posterior median	Bias	Probability of 95% credible intervals containing the true population mean
No transporter scenario					
Low Variability (5% BAV +5% WAV)	$AUC^{\infty}_{0,pl}$	50	56.16	12.3%	1
	$AUC^{\infty}_{0,br}$	50	54.22	8.4%	1
	$\frac{AUC^{\infty}_{0,br}}{AUC^{\infty}_{0,pl}}$	1	0.9694	3.1%	1
Median Variability (10% BAV +10% WAV)	$AUC^{\infty}_{0,pl}$	50	56.39	12.8%	1
	$AUC^{\infty}_{0,br}$	50	54.17	8.3%	1
	$\frac{AUC^{\infty}_{0,br}}{AUC^{\infty}_{0,pl}}$	1	0.9654	3.5%	1
High Variability 1 (20% BAV +10% WAV)	$AUC^{\infty}_{0,pl}$	50	57.89	15.8%	0.998
	$AUC^{\infty}_{0,br}$	50	54.42	8.8%	1
	$\frac{AUC^{\infty}_{0,br}}{AUC^{\infty}_{0,pl}}$	1	0.9473	5.3%	1
High Variability 2 (20% BAV +20% WAV)	$AUC^{\infty}_{0,pl}$	50	57.42	14.8%	0.997
	$AUC^{\infty}_{0,br}$	50	53.94	7.9%	1
	$\frac{AUC^{\infty}_{0,br}}{AUC^{\infty}_{0,pl}}$	1	0.9476	5.2%	1
High transporter scenario					
Low Variability (5% BAV +5% WAV)	$AUC^{\infty}_{0,pl}$	50	57.78	15.6%	1
	$AUC^{\infty}_{0,br}$	10	11.86	18.6%	1
	$\frac{AUC^{\infty}_{0,br}}{AUC^{\infty}_{0,pl}}$	0.2	0.2058	2.9%	1
Median Variability (10% BAV +10% WAV)	$AUC^{\infty}_{0,pl}$	50	58.07	16.1%	1
	$AUC^{\infty}_{0,br}$	10	11.85	18.5%	1
	$\frac{AUC^{\infty}_{0,br}}{AUC^{\infty}_{0,pl}}$	0.2	0.2048	2.4%	1
High Variability 1 (20% BAV +10% WAV)	$AUC^{\infty}_{0,pl}$	50	59.61	19.2%	0.999
	$AUC^{\infty}_{0,br}$	10	11.89	18.9%	1
	$\frac{AUC^{\infty}_{0,br}}{AUC^{\infty}_{0,pl}}$	0.2	0.2010	0.50%	1
High Variability 2 (20% BAV +20% WAV)	$AUC^{\infty}_{0,pl}$	50	59.07	18.1%	0.998
	$AUC^{\infty}_{0,br}$	10	11.78	17.8%	1
	$\frac{AUC^{\infty}_{0,br}}{AUC^{\infty}_{0,pl}}$	0.2	0.2013	0.65%	1

BAV and WAV had little impact on the estimation bias under the serial sacrifice design. The proportions of simulations in which the true population mean was covered by the 95% credible interval are also shown in Table II. At all tested levels of variability, the Bayesian 95% credible interval had a good coverage rate (above 99%) of the true population mean.

Based on the simulation of extreme-case scenarios that either excluded the tissue efflux transporter activity or included a transporter with high activity, the Bayesian approach was able to adequately handle the parameters $AUC^{\infty}_{0,pl}$, $AUC^{\infty}_{0,br}$ and $\frac{AUC^{\infty}_{0,br}}{AUC^{\infty}_{0,pl}}$ and performs well for a variety of physiological animal models (Table II).

Case Study

The Bayesian NCA approach has been applied to the brain distribution study of cediranib in wild-type and gene-knockout mice of brain efflux transporters, such as P-gp and BCRP; see more details in our experimental work (23). The aim of the animal pharmacokinetic study was to compare the cediranib

brain partitioning among different genotypes in order to explore the role of brain efflux transporters in the brain penetration of cediranib, an *in vitro* substrate of P-gp and BCRP. Based on the Bayesian approach, the posterior medians and 95% credible intervals of the cediranib plasma and brain AUC_0^∞s and $\frac{AUC^\infty_{0,br}}{AUC^\infty_{0,pl}}$ in the wild-type, *Mdr1a/b(-/-)*, *Bcrp1(-/-)*, and *Mdr1a/b(-/-) Bcrp1(-/-)* mice were listed on Table III. The posterior distributions of the cediranib DTIs $\left(\frac{\left(\frac{AUC^\infty_{0,br}}{AUC^\infty_{0,pl}}\right)_{transgenic\cdot mice}}{\left(\frac{AUC^\infty_{0,br}}{AUC^\infty_{0,pl}}\right)_{wildtype\cdot mice}}\right)$ for *Mdr1a/b(-/-)*, *Bcrp1(-/-)*, and *Mdr1a/b (-/-) Bcrp1(-/-)* mice were also shown in the kernel density plots (Fig. 4). The results confirmed the hypothesis that P-gp might play a predominant role in excluding cediranib out of the brain, based on the fact that the cediranib DTI in the *Mdr1a/b(-/-)* and *Mdr1a/b(-/-) Bcrp1(-/-)* mice were approximately 20-fold higher than the *Bcrp1(-/-)* mice.

The Bayesian estimators of $\frac{AUC^\infty_{0,br}}{AUC^\infty_{0,pl}}$ were compared to Yuan's approximation and jackknife estimation in Table III. The posterior medians of the $AUC^\infty_{0,pl}$, $AUC^\infty_{0,br}$ and $\frac{AUC^\infty_{0,br}}{AUC^\infty_{0,pl}}$ in different mice groups were very similar to the point estimate by Yuan's method and by jackknife resampling, with all differences ≤14%. As expected, the Bayesian 95% credible intervals of $AUC^\infty_{0,pl}$ and $AUC^\infty_{0,br}$ were slightly wider than the 95% confidence intervals approximated by Yuan's method. The Bayesian 95% credible intervals of $AUC^\infty_{0,pl}$, $AUC^\infty_{0,br}$ and $\frac{AUC^\infty_{0,br}}{AUC^\infty_{0,pl}}$ were also slightly wider than the 95% confidence intervals obtained with jackknife resampling.

The precision of Bayesian credible intervals for the estimated plasma and brain AUC_0^t was compared to the classic Bailer-type confidence intervals. Table IV shows that the Bayesian posterior medians of $AUC_0{}^t$ in those mice groups were very close to the means (differences <15%) estimated by the Bailer-Satterthwaite method with the Bayesian 95% credible interval coverage similar to the 95% Bailer-type confidence intervals.

DISCUSSION

In a serial sacrifice tissue penetration study, assessing the estimation precision of AUC-based parameters such as partition coefficient and DTI is often desired. Since the plasma and tissue concentrations at the same time point are usually measured in the same animal, the correlation between the plasma and tissue concentrations may not be ignored. The biggest advantage of our proposed Bayesian NCA approach over most commonly used Bailer-type methods is its capability in

Table III Bayesian Posterior Median and 95% Credible Interval (C.I.) of the Plasma and Brain $AUC_0{}^\infty$ and Their Ratios after Intravenous Dose of 4 mg/kg Cediranib in Wild-type (WT), *Bcrp1(-/-)* (BCRPKO), *Mdr1a/b(-/-)* (PgpKO) and *Mdr1a/b(-/-)Bcrp1(-/-)* (TKO) Mice, and the Comparison with the Point Estimate and 95% Confidence Interval (C.I.*) Estimated with the Bailer-based Approximation Extended by Yuan and with the Jackknife Resampling Approach

Parameter	Bayesian estimation		Yuan's extention of Bailer's method		Jackknife resampling ($N = 1{,}000$)	
	Posterior median	95% C.I.	Mean	95% C.I.*	Mean	95% C.I.*
$AUC^\infty_{0,pl,WT}$	9,758	(8,883, 10,720)	9,697	(9,295, 10,099)	9,741	(9,311, 10,151)
$AUC^\infty_{0,br,WT}$	2,652	(2,252, 3,085)	2,661	(2,561, 2,761)	2,750	(2,586, 2,930)
$AUC^\infty_{0,pl,BCRPKO}$	11,420	(9,446, 15,780)	10,220	(8,748, 11,692)	10,596	(9,401, 12,071)
$AUC^\infty_{0,br,BCRPKO}$	2,090	(1,805, 2,414)	1,997	(1,915, 2,079)	2,049	(1,906, 2,175)
$AUC^\infty_{0,pl,PgpKO}$	7,753	(7,140, 8,351)	7,785	(7,558, 8,012)	7,752	(7,462, 8,016)
$AUC^\infty_{0,br,PgpKO}$	52,460	(50,290, 54,540)	52,560	(51,751, 53,369)	53,947	(53,043, 54,908)
$AUC^\infty_{0,pl,TKO}$	9,581	(8,690, 10,500)	8,408	(8,163, 8,653)	8,622	(8,166, 8,974)
$AUC^\infty_{0,br,TKO}$	53,500	(48,960, 58,080)	51,966	(50,733, 53,199)	52,564	(50,533, 54,686)
$\left(\frac{AUC^\infty_{0,br}}{AUC^\infty_{0,pl}}\right)_{WT}$	0.27	(0.24, 0.31)	0.27	–	0.28	(0.26, 0.31)
$\left(\frac{AUC^\infty_{0,br}}{AUC^\infty_{0,pl}}\right)_{BCRPKO}$	0.18	(0.13, 0.22)	0.20	–	0.19	(0.17, 0.22)
$\left(\frac{AUC^\infty_{0,br}}{AUC^\infty_{0,pl}}\right)_{PgpKO}$	6.77	(6.30, 7.30)	6.75	–	6.96	(6.70, 7.24)
$\left(\frac{AUC^\infty_{0,br}}{AUC^\infty_{0,pl}}\right)_{TKO}$	5.59	(5.22, 5.97)	6.18	–	6.10	(5.75, 6.54)

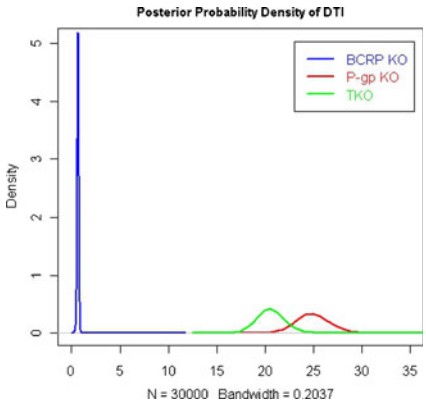

Fig. 4 Posterior distributions of the brain drug targeting index (DTI) for the three transporter knockout mice. *Blue*: *Bcrp1(-/-)* mice; *Red*: *Mdr1a/b(-/-)* mice; *Green*: *Mdr1a/b(-/-)Bcrp1(-/-)* mice.

evaluating the precision of AUC-based parameters of interest in a serial sacrifice design based on their posterior distributions. Unlike other approaches, this approach also inherently takes into account the correlation between tissue and plasma when calculating the plasma and tissue AUC.

Our approach does not rely on any compartmental assumption but the first-order kinetics assumption of the terminal elimination phase. The simulation and case study in the model assumed linear distributional kinetics, *i.e.*, no saturation of the efflux clearance processes. However, the data analysis method to determine the statistical differences in the $\frac{AUC^{\infty}_{0,br}}{AUC^{\infty}_{0,pl}}$ would still be valid in the case of saturation of efflux, however the inference as to why the AUC ratios differ may be affected.

Bayesian credible intervals allow direct probability statements on the uncertainty of a parameter estimate (25). It has been shown that the posterior median is a robust estimator for data with non-symmetric distributions, such as multimodal or skewed distributions (26). Since the elimination phase rate constant was determined based on the assumption that terminal phase concentration data follow the log-normal distribution, the tail behavior of the non-symmetric distribution may affect the simulation-based sampling. That was the reason why the posterior median was used as a preferred estimator, along with the credible interval.

The performance of the Bayesian approach for $AUC^{\infty}_{0,pl}$, $AUC^{\infty}_{0,br}$, and $\frac{AUC^{\infty}_{0,pl}}{AUC^{\infty}_{0,pl}}$ in 1,000 simulated data sets with different levels of variability suggested that the Bayesian NCA approach is accurate and precise in the estimation of AUC^{∞}_{0} and the tissue-to-plasma partition coefficient for serial sacrifice designs. The simulations indicated that the Bayesian credible interval gave good coverage of the population parameter, a known quantity. The robustness of the application of this approach does not rely on the variability of the data or the physiological structure of the pharmacokinetic model.

In the case study, the Bayesian estimators of the plasma and brain AUC^{∞}_{0}s were compared with the point estimates and 95% confidence intervals estimated by the Bailer's approximation extended by Yuan and by jackknife resampling. The Bayesian posterior median and 95% credible intervals of brain-to-plasma partition coefficients were also compared to the jackknife mean and 95% confidence intervals. Yuan's method provided tighter confidence intervals than the Bayesian approach, since Yuan's method inherently underestimates the variance of AUC^{∞}_{0} because of its double usage of the last sampling time point for estimation of λ_z and calculation of the AUC from the last sampling time up to infinity (15). Although in the Bayesian approach, the observed data at the last sampling time were used in determination of posterior distributions of both C_t and λ_z, the samplings of λ_z and C_t were separated. Hence, it was anticipated that the Bayesian credible intervals are wider than the Yuan's confidence intervals. It is also not surprising that the jackknife confidence intervals were also narrower than the Bayesian credible intervals when the sample size is extremely small (*e.g.*, in our case, only four replicates at each time point). However, this derived jackknife intervals might not be reliable. As Efron points out, resampling intervals are not exact and may sometimes be vulnerable in small-sample situations (20). In contrast, Bayesian approach in nature can avoid the dilemma of frequentist point estimation caused by the small sample size. The posterior distributions of the parameters of interest depend on both prior settings and study data, and small sample size is usually not an issue in Bayesian analysis. As such, our proposed approach is robust and adequate in the case study. Moreover, our approach considers the brain and plasma data

Table IV Comparisons of Bayesian Posterior Median and 95% Credible Interval (C.I.) for the Plasma and Brain $AUC_0{}^t$ after Intravenous Dose of 4 mg/kg Cediranib in Wild-type (WT), *Bcrp1(-/-)* (BCRPKO), *Mdr1a/b(-/-)* (PgpKO) and *Mdr1a/b(-/-)Bcrp1(-/-)* (TKO) Mice with Bailer-Satterthwaite Approximation of Mean and 95% Confidence Interval (C.I.*) Estimated by Phoenix WinNonlin®

Parameter	Bayesian estimation		Bailer-Satterthwaite estimation	
	Posterior median	95% C.I.	Mean	95% C.I.*
$AUC^{t}_{0,pl,WT}$	9,208	(8,386, 10,090)	9,200	(8,487, 9,913)
$AUC^{t}_{0,br,WT}$	2,455	(2,066, 2,879)	2,449	(2,131, 2,767)
$AUC^{t}_{0,pl,BCRPKO}$	9,494	(8,240, 10,830)	8,393	(7,634, 9,152)
$AUC^{t}_{0,br,BCRPKO}$	2,030	(1,750, 2,343)	1,947	(1,726, 2,168)
$AUC^{t}_{0,pl,PgpKO}$	7,384	(6,774, 7,980)	7,396	(6,920, 7,872)
$AUC^{t}_{0,br,PgpKO}$	48,160	(46,120, 50,110)	48,186	(46,604, 49,768)
$AUC^{t}_{0,pl,TKO}$	9,490	(8,603, 10,410)	8,307	(7,509, 9,105)
$AUC^{t}_{0,br,TKO}$	52,710	(48,170, 57,220)	51,107	(47,348, 54,866)

correlation in model setting, which is another big advantage over the other methods. Although resampling maintains the data correlation between tissue and plasma within same animals, the AUC calculation based on resampling approaches is still unable to account for the tissue-and-plasma correlation, since presumably, the tissue and plasma AUCs are calculated independently.

In parallel, the point estimates and the Bailer-type confidence intervals for the AUC_0^t s were compared to the Bayesian posterior medians and credible intervals in the case study. The purpose of the comparison was simply to show that the non-informative Bayesian method produced physiologically reasonable parameter estimations. Since the way Bayesian approach determines the terminal elimination phase was slightly different from Phoenix WinNonlin®, AUC_0^∞ was not selected as a parameter to compare with the Phoenix WinNonlin® calculation results. Phoenix WinNonlin® calculates the terminal phase rate constant by repeating regressions using the last three points then the last four points, last five, *etc.*, until obtaining the best linear fit (27). But the current study used only the last three time points with non-zero concentrations for the purpose of computation simplicity. Instead of AUC_0^∞, the estimated AUC_0^t was compared. Results showed that the Bayesian posterior estimates of the AUC_0^t in the four different mice models were very close to the mean and 95% confidence interval estimated by the Bailer-Satterthwaite method with Phoenix WinNonlin®.

One criticism on the application of the Bayesian method is that the setting of the prior distribution is subjective and different priors may yield different posterior results. But the use of non-informative priors (*e.g.*, the uniform prior for log-concentration means) in this work can make this "subjectivity" minimal. Furthermore, incorporation of informative priors under some circumstances may be very helpful to investigate parameters. The Bayesian approach provides a flexible and powerful tool to borrow strength from other studies.

In the present simulation, the error at each sampling time was assumed to follow a log-normal distribution (proportional to the mean value of concentrations). Thus, the concentration data were log-transformed and the entire analysis was done on a log-scale. In the animal study, the normal likelihood worked adequately well and no significant difference between the normal likelihood and the log-normal likelihood was in that case. Other appropriate assumptions of likelihood and priors are worth exploring in further studies. However, when prior knowledge is available, it is strongly recommended to incorporate informative priors into the Bayesian approach. This will help narrow down the credible intervals of the Bayesian estimate and generate a more reliable posterior distribution. Another disadvantage of the Bayesian NCA approach is that it requires knowledge of Bayesian statistics and that the programming may be difficult to a non-statistician. The OpenBUGS code used in this analysis is included in the Supplementary Material.

CONCLUSION

Our proposed Bayesian approach provides a useful tool for variance estimation of the AUC_0^∞, the tissue-to-plasma ratio of AUC_0^∞, and the DTI, following destructive sampling. Posterior distribution of other NCA parameters could be obtained in likewise fashion. When prior knowledge is available, it is strongly recommended to incorporate informative priors into the Bayesian approach, in order to obtain a more reliable posterior estimation.

ACKNOWLEDGMENTS AND DISCLOSURES

This work was supported by National Institutes of Health grants CA 138437, and NS 077921.

REFERENCES

1. Dallas CE, Chen XM, O'Barr K, Muralidhara S, Varkonyi P, Bruckner JV. Development of a physiologically based pharmacokinetic model for perchloroethylene using tissue concentration-time data. Toxicol Appl Pharmacol. 1994;128:50–9.
2. Meno-Tetang GM, Li H, Mis S, Pyszczynski N, Heining P, Lowe P, *et al*. Physiologically based pharmacokinetic modeling of FTY720 (2-amino-2[2-(-4-octylphenyl)ethyl]propane-1,3-diol hydrochloride) in rats after oral and intravenous doses. Drug Metab Dispos Biol Fate Chem. 2006;34:1480–7.
3. Wang T. Mechanisms and analysis of the CNS distribution of cediranib, a molecularly-targeted anti-angiogenic agent., *Doctoral Dissertation*, University of Minnesota, 2011.
4. Siegel RA, MacGregor RD, Hunt CA. Comparison and critique of two models for regional drug delivery. J Pharmacokinet Biopharm. 1991;19:363–73. discussion 373-364.
5. Stevens AJ, Martin SW, Brennan BS, McLachlan A, Gifford LA, Rowland M, *et al*. Regional drug delivery II: relationship between drug targeting index and pharmacokinetic parameters for three non-steroidal anti-inflammatory drugs using the rat air pouch model of inflammation. Pharm Res. 1995;12:1987–96.
6. Navarro-Fontestad C, Gonzalez-Alvarez I, Fernandez-Teruel C, Bermejo M, Casabo VG. A new mathematical approach for the estimation of the AUC and its variability under different experimental designs in preclinical studies. Pharm Stat. 2012;11(1):14–23.
7. Berry DA. Bayesian clinical trials. Nat Rev Drug Discov. 2006;5:27–36.
8. Spiegelhalter DJ, Abrams KR, Myles JP. Bayesian approaches to clinical trials and health-care evaluation, Wiley. com, 2004.
9. Zhong W, Koopmeiners JS, Carlin BP. A trivariate continual reassessment method for phase I/II trials of toxicity, efficacy, and surrogate efficacy. Stat Med. 2012;31:3885–95.
10. Zhong W, Koopmeiners JS, Carlin BP. A two-stage Bayesian design with sample size reestimation and subgroup analysis for phase II binary response trials. Contemporary Clinical Trials 2013.

11. Lunn DJ, Best N, Thomas A, Wakefield J, Spiegelhalter D. Bayesian analysis of population PK/PD models: general concepts and software. J Pharmacokinet Pharmacodyn. 2002;29:271–307.
12. Jelliffe R, Neely M, Schumitzky A, Bayard D, Van Guilder M, Botnen A, et al. Nonparametric population modeling and Bayesian analysis. Pharmacol Res. 2011.
13. Bailer AJ. Testing for the equality of area under the curves when using destructive measurement techniques. J Pharmacokinet Biopharm. 1988;16:303–9.
14. Nedelman JR, Gibiansky E, Lau DT. Applying Bailer's method for AUC confidence intervals to sparse sampling. Pharm Res. 1995;12:124–8.
15. Yuan J. Estimation of variance for AUC in animal studies. J Pharm Sci. 1993;82:761–3.
16. Bonate PL. Coverage and precision of confidence intervals for area under the curve using parametric and non-parametric methods in a toxicokinetic experimental design. Pharm Res. 1998;15:405–10.
17. Jaki T, Wolfsegger MJ, Ploner M. Confidence intervals for ratios of AUCs in the case of serial sampling: a comparison of seven methods. Pharm Stat. 2009;8:12–24.
18. Wolfseggerand MJ, Jaki T. Estimation of AUC from 0 to infinity in serial sacrifice designs. J Pharmacokinet Pharmacodyn. 2005; 32:757–66.
19. Wolfseggerand MJ, Jaki T. Non-compartmental estimation of pharmacokinetic parameters in serial sampling designs. J Pharmacokinet Pharmacodyn. 2009;36:479–94.
20. Efron B. Second thoughts on the bootstrap. Stat Sci. 2003;18:135–40.
21. Thomas A. BRugs user manual, version 1.0. Dept of Mathematics & Statistics, University of Helsinki 2004.
22. R.Development.Core.Team. R: A language and environment for statistical computing, R Foundation for Statistical Computing, Vienna, Austria, 2010.
23. Wang T, Agarwal S, Elmquist WF. Brain distribution of cediranib is limited by active efflux at the blood-brain barrier. J Pharmacol Exp Ther. 2012;341:386–95.
24. Nedelmanand JR, Jia X. An extension of Satterthwaite's approximation applied to pharmacokinetics. J Biopharm Stat. 1998;8:317–28.
25. Carlinand BP, Louis TA. Bayes and empirical Bayes methods for data analysis. Stat Comput. 1997;7:153–4.
26. Bochkinaand N, Sapatina T. On the posterior median estimators of possibly sparse sequences. Ann Inst Statist Math. 2005;57:315–51.
27. Phoenix. WinNonlin™, Certara Coperation at St. Louis, MI.